# Supplemental Figures

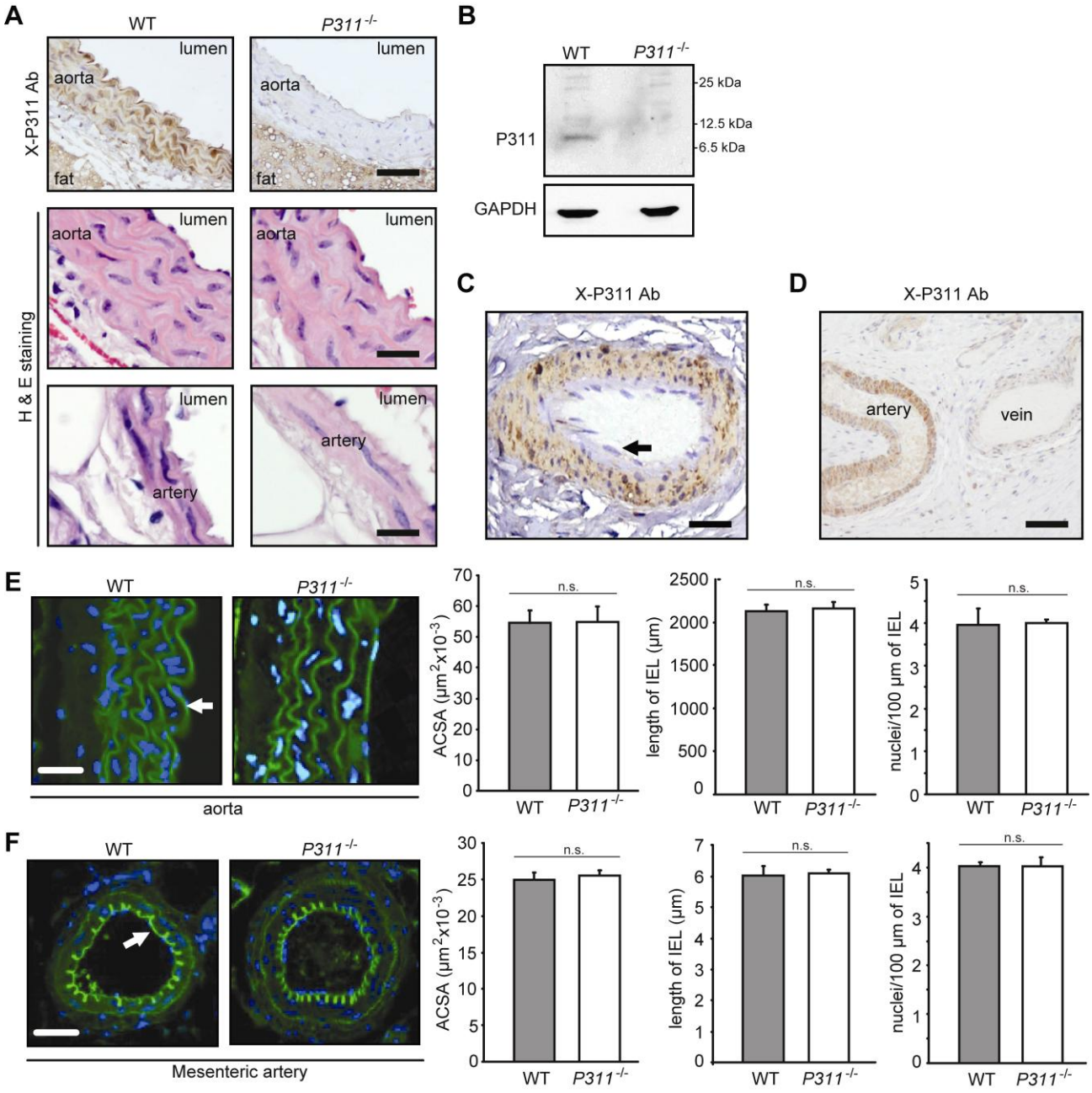


**Supplemental Figure 1** Presence of P311 in mouse and human vascular muscle. (**A**) P311 immunoreactivity (brown staining) in WT and *P311*$^{-/-}$ mice aortas in upper two panels. Hematoxylin and eosin staining (H&E) showing nuclei (blue staining) and eosinophilic structure (pink staining) in bottom four panels. Scale bars, 50 μm in upper two panels and 10 μm in the rest. (**B**) Western blot analysis of P311 in WT and *P311*$^{-/-}$ mice aortas. (**C**) P311 immunoreactivity (brown staining) in human artery. Arrow indicates endothelium. Scale bar, 40 μm. (**D**) P311 immunoreactivity (brown staining) in human artery and vein. Scale bar, 100 μm. (**E** and **F**) Morphometry images, anatomic cross-sectional area (ACSA), length of internal elastic lamina (IEL) and number of nuclei comprised between two elastic laminas in the aortas (**E**) and mesenteric arteries (**F**) from WT and *P311*$^{-/-}$ mice. Arrows indicate elastic lamina. Scale bars, 25 μm for aorta and 50 μm for mesenteric artery. Data represent mean ± s.d. n.s., non-significant by one-way ANOVA.

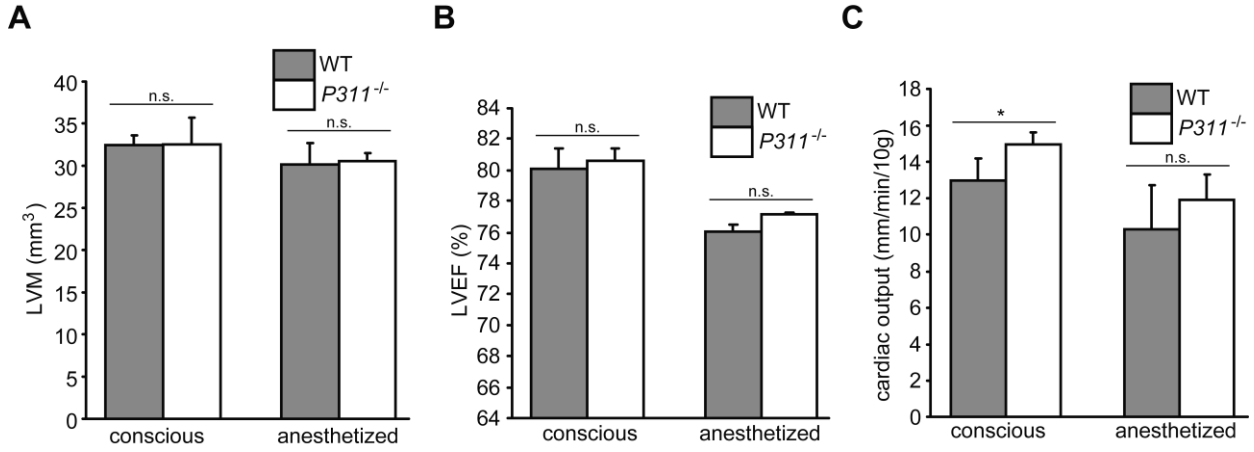


**Supplemental Figure 2** *P311*$^{-/-}$ mice have normal heart function. Transthoracic echocardiography parameters of WT and *P311*$^{-/-}$ mice. (**A**) Left ventricular mass (LVM). (**B**) Left ventricular ejection fraction (LVEF). (**C**) Cardiac output. Data represent mean ± s.d. **p* < 0.05, n.s., non-significant by one-way ANOVA.

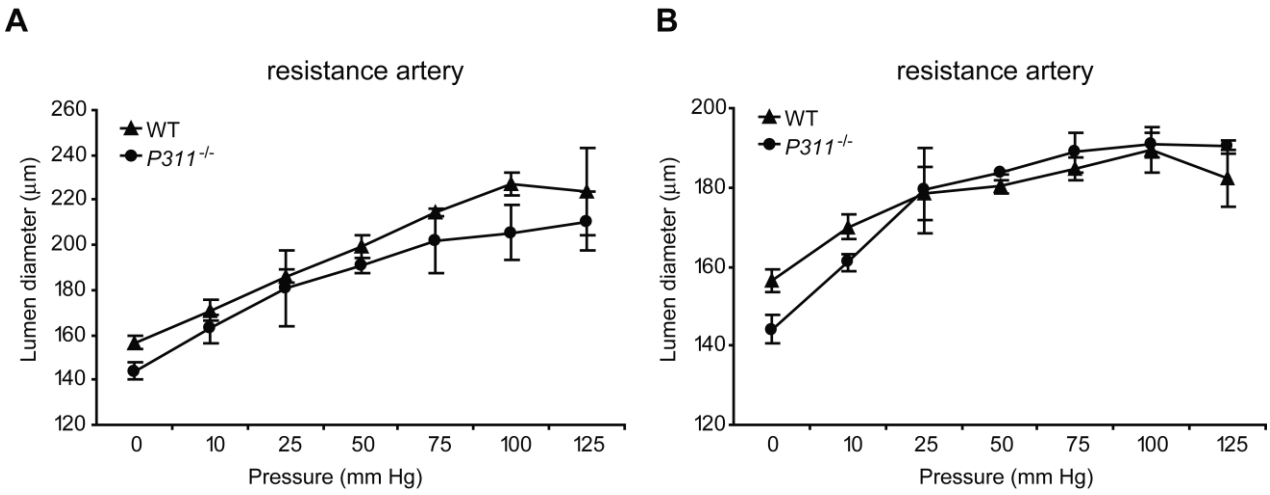


**Supplemental Figure 3** Artery lumen diameters of WT and *P311*$^{-/-}$ mice determined by pressure myograph. (**A**) Passive artery lumen diameter curve determined in $Ca^{2+}$-free PSS buffer. (**B**) Active artery lumen diameter curve determined in PSS buffer (containing 2.5 mM $CaC1_2$).

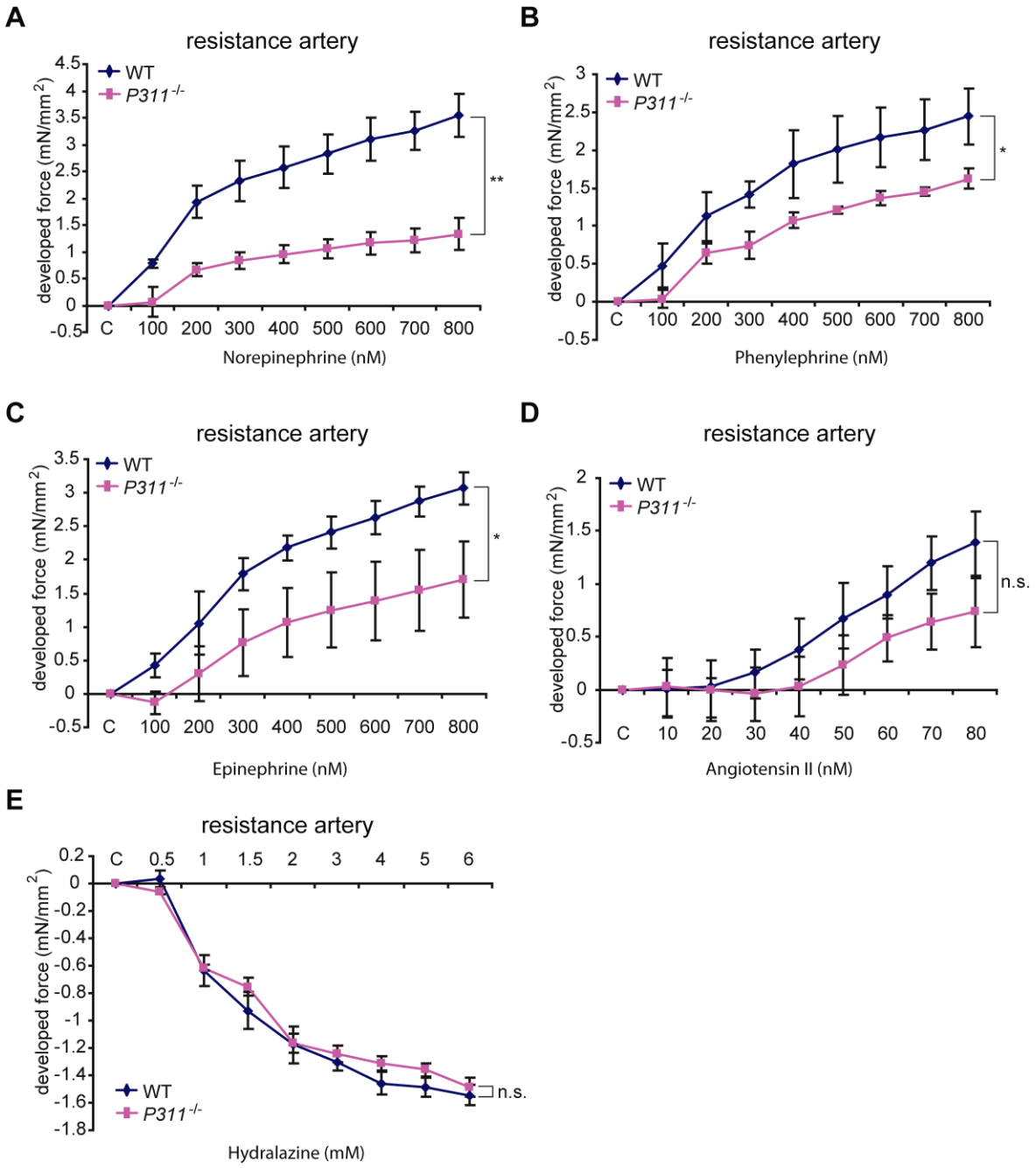


**Supplemental Figure 4** Myographic determination of the contractile and dilatational response of isolated resistance arteries (~100 µm in diameter) from WT ($n$ = 3) and P311$^{-/-}$ ($n$ = 3) mice to vasoconstrictors and vasodilator. (**A**) Norepinephrine. (**B**) Phenylephrine. (**C**) Epinephrine. (**D**) Angiotensin II. (**E**) Hydralazine. Data at final time points were statistically analyzed by one-way ANOVA. Data represent mean ± s.d. *$p < 0.05$, **$p < 0.01$, n.s., non-significant.

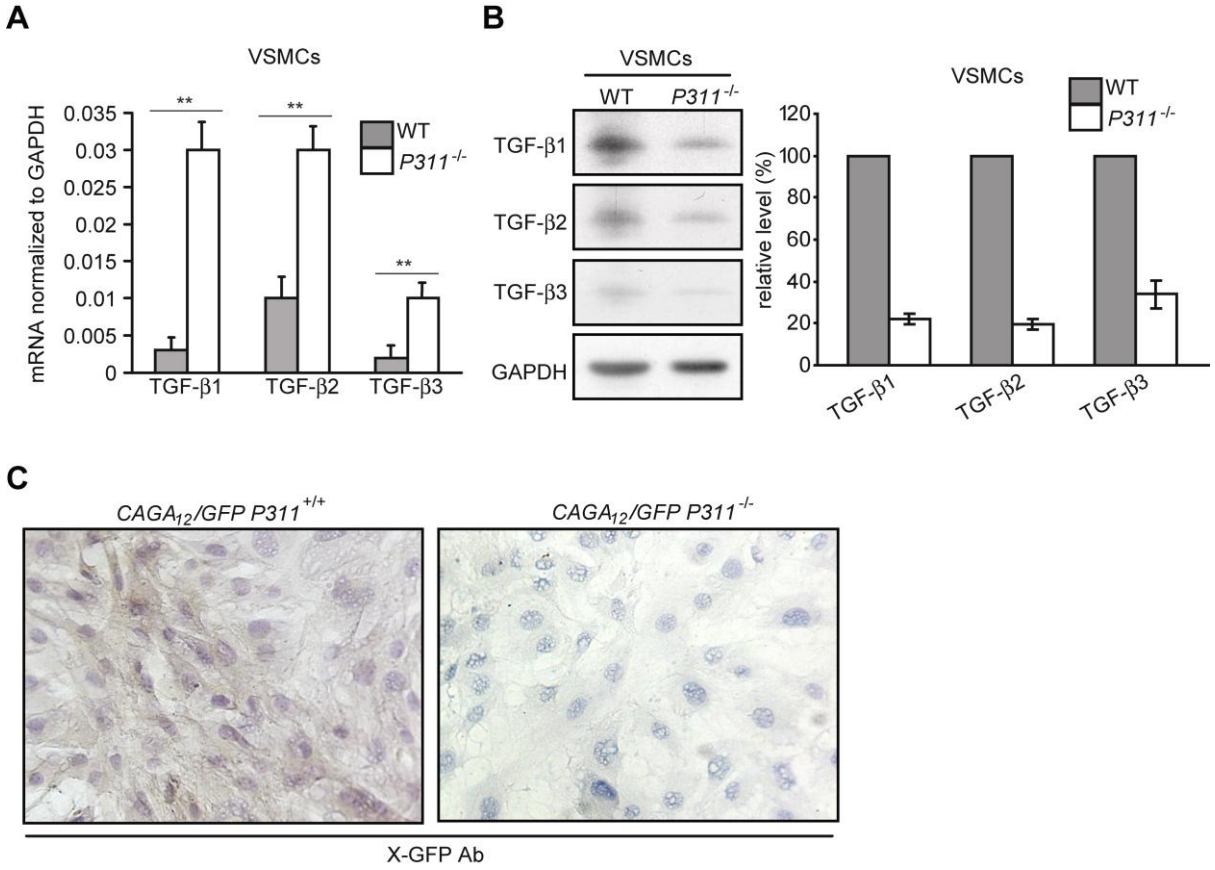


**Supplemental Figure 5** VSMCs isolated from *P311*$^{-/-}$ mice have a decrease in the level and activity of TGF-β1, 2 and 3 and their preforms but not in the corresponding mRNAs. (**A**) Real-time PCR showing mRNA levels of TGF-βs in WT and *P311*$^{-/-}$ mice aortic VSMCs. Data represent mean ± s.d. $^{**}p < 0.01$ by one-way ANOVA. (**B**) Western blots showing TGF-βs in VSMCs from WT and *P311*$^{-/-}$ mice. The relative level of TGF-βs in *P311*$^{-/-}$ VSMCs is shown in the histogram on the right as compared with WT VSMCs. (**C**) GFP immunoreactivity (brown staining) in *CAGA*$_{12}$*/GFP* transgenic *P311*$^{+/+}$ and *P311*$^{-/-}$ mice VSMCs.

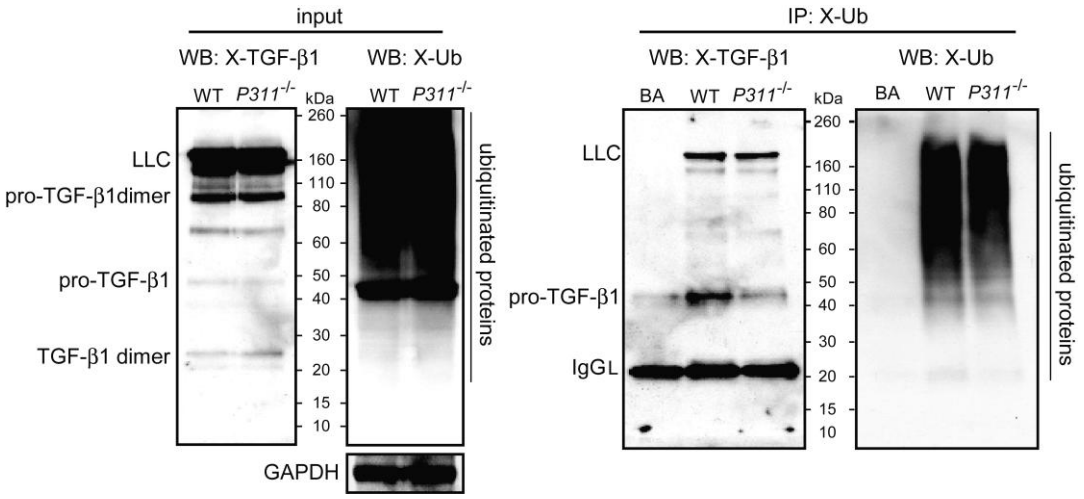


**Supplemental Figure 6** P311 shows no effect on TGF-β1 ubiquitination. Ubiquitin (Ub) immunoprecipitation (IP) assays and western blots (WB) showing the ubiquitinated TGF-β1 in aortas. Input was normalized according to TGF-β1 level in WT and *P311*$^{-/-}$ mice aortas. Equal amount of total ubiquitinated protein was immunoprecipitated from normalized input for TGF-β1 detection. LLC, large latent TGF-β complex. BA, beads alone.

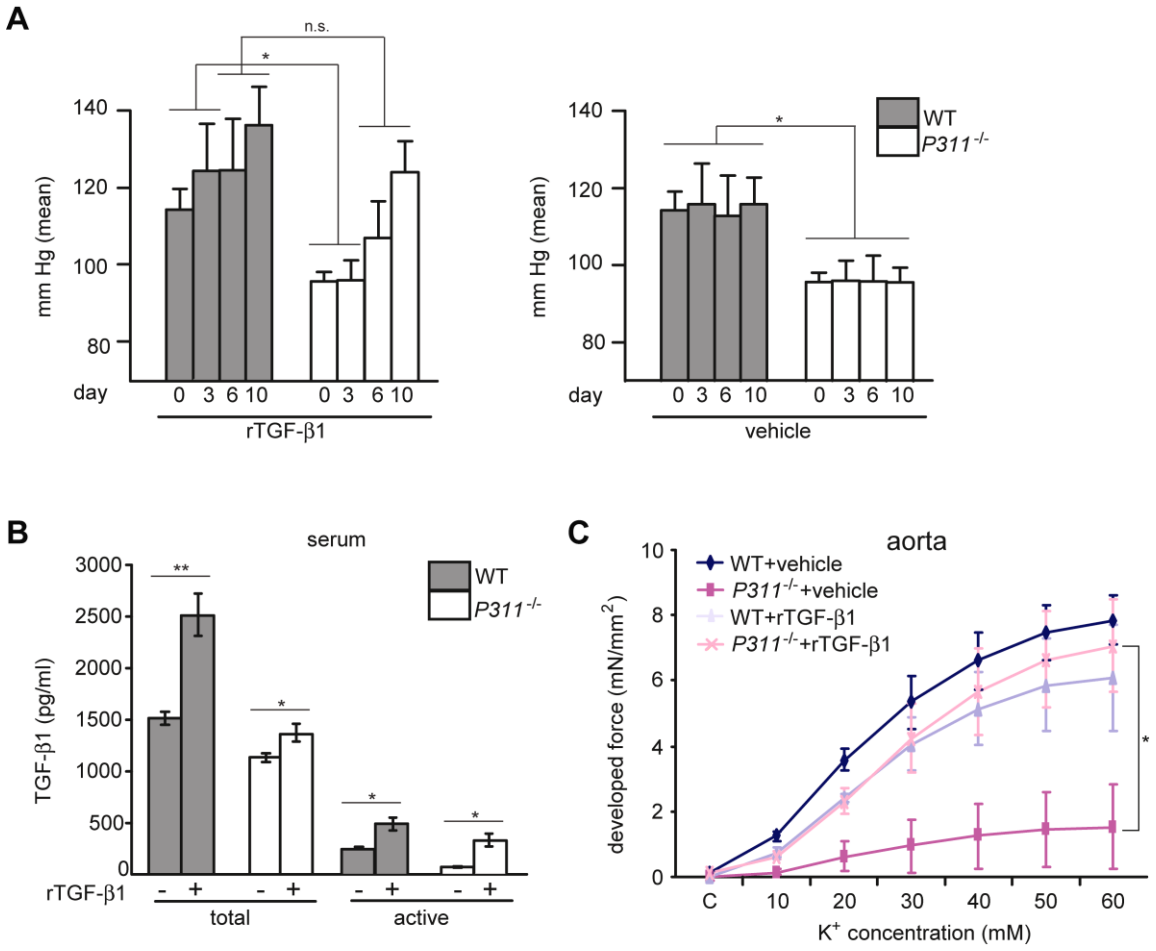


**Supplemental Figure 7** Administration of rTGF-β1 to *P311*$^{-/-}$ mice improves blood pressure and contractility. (**A**) Plethysmographic blood pressure determination in WT ($n$ = 5) and *P311*$^{-/-}$ ($n$ = 5) mice, with and without rTGF-β1 treatment. (**B**) ELISA showing total and active TGF-β1 in WT ($n$ = 4) and *P311*$^{-/-}$ ($n$ = 4) mice blood serum, with and without rTGF-β1 treatment. (**C**) Contractile response of aortas from WT ($n$ = 5) and *P311*$^{-/-}$ mice ($n$ = 5) to increasing $K^+$ concentration, with and without rTGF-β1 treatment. Data represent mean ± s.d. *$p < 0.05$, **$p < 0.01$, n.s., non-significant by one-way ANOVA.

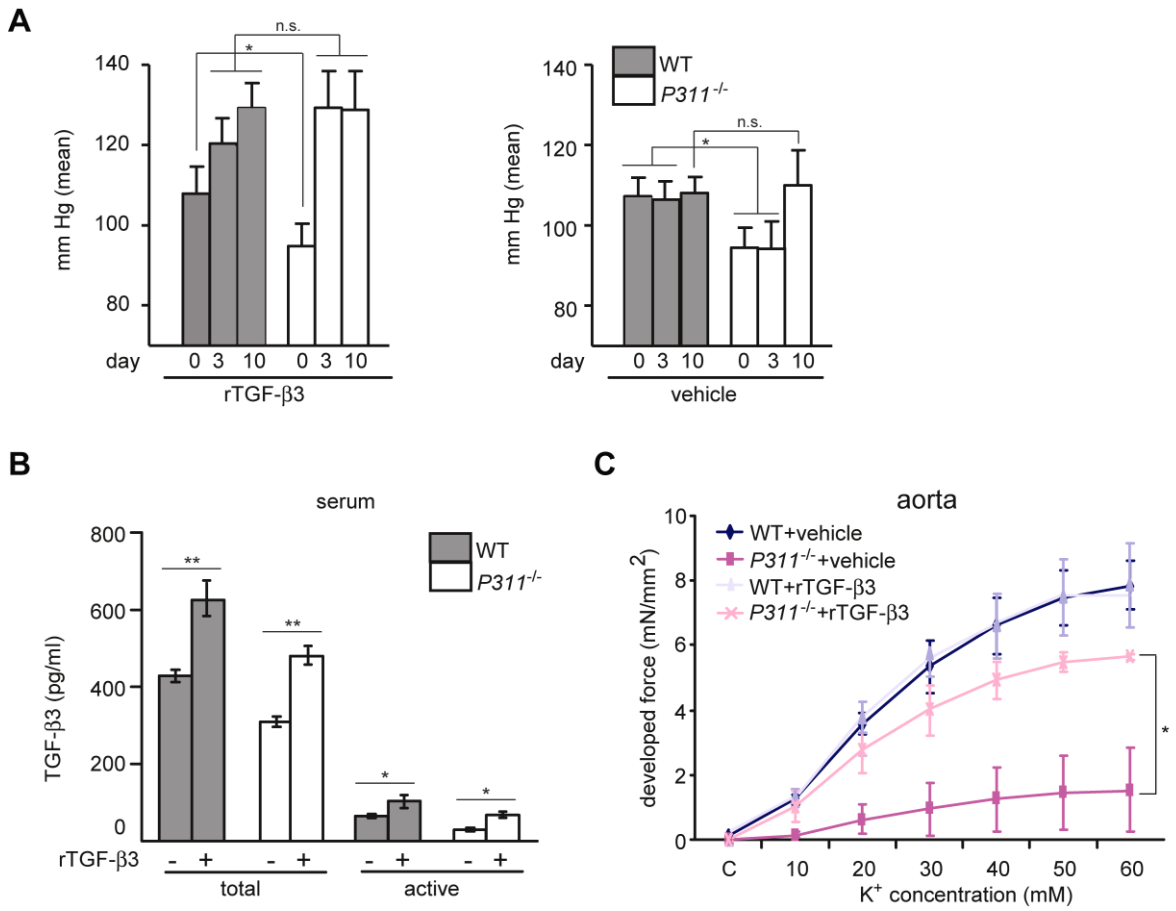


**Supplemental Figure 8** Administration of rTGF-β3 to *P311*$^{-/-}$ mice improves blood pressure and contractility. (**A**) Plethysmographic blood pressure determination in WT ($n$ = 5) and *P311*$^{-/-}$ ($n$ = 5) mice, with and without rTGF-β1 treatment. (**B**) ELISA showing total and active TGF-β3 in WT ($n$ = 4) and *P311*$^{-/-}$ ($n$ = 4) mice blood serum, with and without rTGF-β3 treatment. (**C**) Contractile response of aortas from WT ($n$ = 5) and *P311*$^{-/-}$ mice ($n$ = 5) to increasing $K^+$ concentration, with and without rTGF-β3 treatment. Data represent mean ± s.d. *$p < 0.05$, **$p < 0.01$, n.s., non-significant by one-way ANOVA.

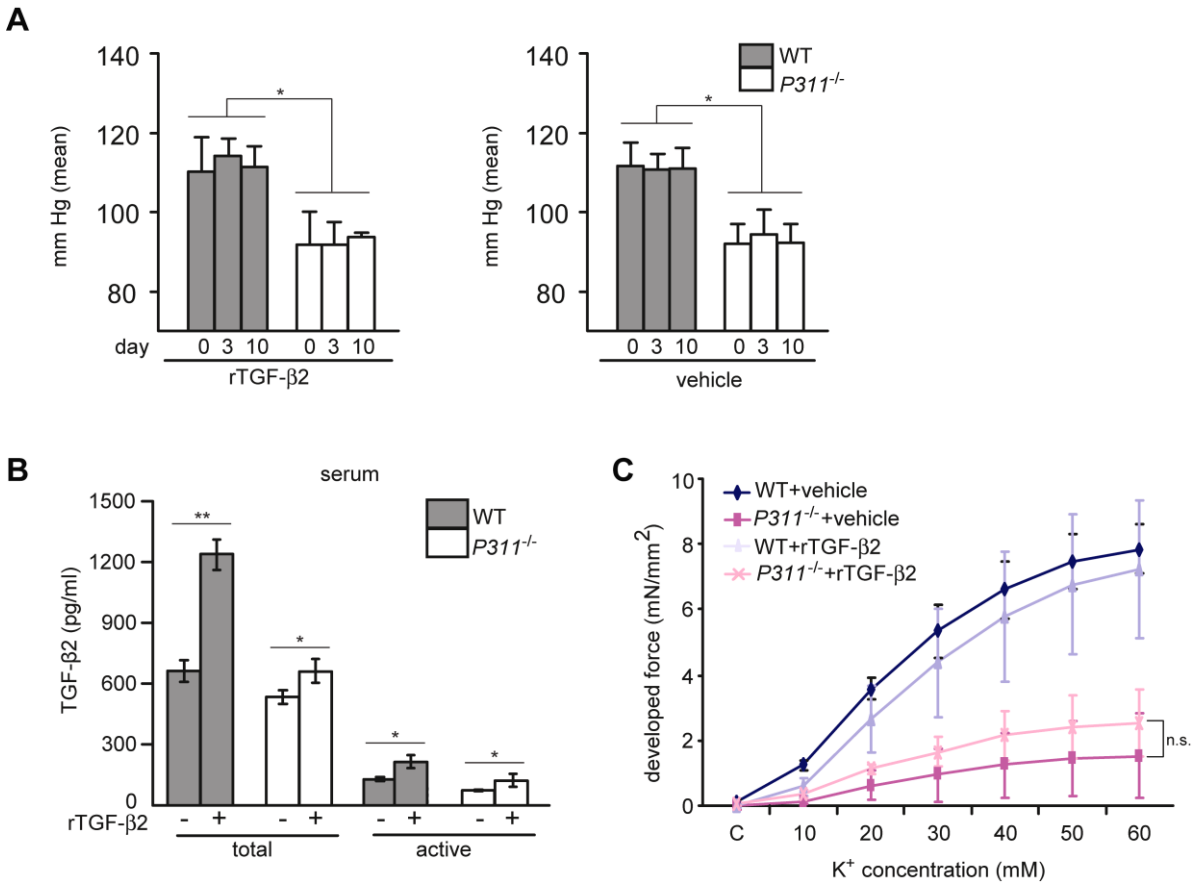


**Supplemental Figure 9** Administration of rTGF-β2 to *P311*$^{-/-}$ mice does not improve blood pressure and contractility. (**A**) Plethysmographic blood pressure determination in WT ($n$ = 5) and *P311*$^{-/-}$ ($n$ = 5) mice, with and without rTGF-β2 treatment. (**B**) ELISA showing total and active TGF-β2 in WT ($n$ = 4) and *P311*$^{-/-}$ ($n$ = 4) mice blood serum, with and without rTGF-β2 treatment. (**C**) Contractile response of aortas from WT ($n$ = 5) and *P311*$^{-/-}$ mice ($n$ = 5) to increasing $K^+$ concentration, with and without rTGF-β2 treatment. Data represent mean ± s.d. *$p < 0.05$, **$p < 0.01$, n.s. non-significant by one-way ANOVA.